The 6th International Conference on
Structural Health Monitoring of Intelligent Infrastructure
Hong Kong | 9-11 December 2013

IMPROVING REMAINING-FATIGUE-LIFE EVALUATION USING DATA INTERPRETATION

Romain Pasquier, Yves Reuland And Ian F.C. Smith
Applied Computing and Mechanics Laboratory (IMAC),
School of Architecture, Civil and Environmental Engineering (ENAC),
École Polytechnique Fédérale de Lausanne (EPFL), Lausanne, Switzerland. Email : romain.pasquier@epfl.ch

ABSTRACT

This paper presents a methodology that improves fatigue-performance evaluations using model-based data interpretation. The accuracy of stress-range values is essential for quantifying fatigue damage. These values are usually predicted using physics-based models such as those used within finite element analyses. In the modelling process, simplifications are inevitable, thus causing systematic errors in model predictions. Structural health monitoring coupled with model-based data-interpretation approaches have the potential to reduce uncertainties associated with the evaluation of stress-range predictions. Because of the presence of modelling and measurement uncertainties, many models may explain the true structural behaviour. A model falsification approach, which is able to cope with incomplete knowledge of uncertainties, is used to isolate candidate models from an initial population of models. This approach is robust for systematic errors that are correlated spatially. The candidate models that are identified using the model-falsification approach predict stress ranges in structural members, from which the remaining fatigue life is determined. Due to the uncertainty reduction in model predictions during data interpretation, the accuracy of the fatigue prognosis is improved. A steel beam composed of a circular hollow-section truss is studied for illustration. Monitoring data that is interpreted using a model-falsification methodology shows potential for improving evaluations of remaining fatigue life.

KEYWORDS

Model-based data interpretation, uncertainty reduction, remaining-fatigue-life prediction.

INTRODUCTION

Economic and environmental issues associated with the retrofit and the replacement of existing structures is of growing importance. This creates a demand for new techniques that are able to predict accurately their behaviour in order to reduce uncertainties related to decision making. Structural health monitoring provides useful data for supporting such techniques. During the last decade, leveraging the availability of measuring instruments, many studies have emerged for improving fatigue assessment of existing structures. While monitoring structural behaviour helps reduce uncertainties, measured data alone is not sufficient to evaluate the structural performance. According to Papadimitriou *et al.* (2011), direct measurements are able to provide accurate predictive assessment of structural behaviour, however, the prediction locations are limited to the monitored locations. Thus, behaviour models are necessary to link effects at other locations to causes and further, to make prognoses related to structural performance.

Some studies proposed to evaluate fatigue damage based on stress-range predictions that are calculated using finite-element analyses (Guo *et al.* 2012; Liu *et al.* 2010; Siriwardane *et al.* 2008). However, the finite-element model that is used is validated based on simple comparisons of load-test data with model predictions. This validation does not ensure the accuracy of the model predictions. Model-based data-interpretation techniques are required to make sense of measurement data. Techniques such as model calibration and Bayesian model updating have been used to identify the unknown parameters of models. However, the validity of predictions of a calibrated model is limited to the calibration data (ASME 2006) and thus predictions made using this approach cannot be used for remaining-fatigue-life evaluations. In addition, due to measurement and modelling uncertainties, multiple models explain the true structural behaviour. Bayesian model updating leads to right diagnosis in cases where modelling errors and their dependencies can be described completely by random variables (Cheung and Beck, 2009; Strauss *et al.* 2008; Zhang *et al.* 2011). However, for complex civil structures, models have systematic biases that are correlated spatially and among quantities in unknown ways.

In order to meet these challenges, Goulet and Smith (2011 and 2013) proposed a probabilistic model-falsification approach. This data-interpretation technique that uses population of models has shown to be well-suited for diagnosis of systems where the uncertainty is not defined. However, the result of this technique has never been used to perform structural prognosis.

This paper presents a methodology that improves the remaining-fatigue-life of structures using model-based data interpretation. The methodology takes advantage of a model-falsification approach to identify the true behaviour of structures and further, perform remaining-fatigue-life assessment of critical details. These results are then compared with the design-model provisions in order to quantify the benefit provided by the measurement data.

The next section presents the methodology for remaining-fatigue-life predictions using data interpretation. In the following section, the prognosis methodology is illustrated with a steel beam composed of a circular hollow-section truss that was tested experimentally under fatigue loading.

METHODOLOGY

Error-Domain Model Falsification

Goulet and Smith (2011, 2013) proposed a solution for shortcomings of traditional approaches and specially for situations where the error structure is unknown. This approach is named error-domain model falsification. The physical system is described by a behaviour model $g(.)$, which is created among several possible classes of model. This model has a set of n_p unknown physical parameters $\boldsymbol{\theta} = [\theta_1, \theta_2, \dots, \theta_{n_p}]^T$ describing the uncertainty related to the unknown geometrical and material characteristics of the structure, as well as the uncertainty on the connections and the support conditions. Error-domain model falsification compares predicted and measured values. Eq. 1 gives the general formulation that is used to compare predicted and measured quantities.

$$g_i(\boldsymbol{\theta}) - \epsilon^*_{model,i} = y_i - \epsilon^*_{measure,i} \quad (1)$$

The discrepancy between the predicted value $g_i(\boldsymbol{\theta})$ and the observed value y_i represents the observed residual, where i corresponds to the location where these values are compared ($i \in \{1, \dots, n_m\}$). Model errors ($\epsilon^*_{model,i}$) and measurement errors ($\epsilon^*_{measure,i}$) are represented by the random variables $U_{model,i}$ and $U_{measure,i}$. The combination of these uncertainties determines a random variable $U_{C,i}$ describing possible outcomes of the differences between predicted and measured values.

A model instance is falsified if, for any measurement location, the observed residual is outside the interval defined by threshold bounds $[T_{low,i}, T_{high,i}]$ (see Eq. 2). A model instance is thus accepted only if this residual lies inside the bounds at every location i.

$$\forall i \in \{1, \dots, n_m\}: T_{low,i} \leq g_i(\boldsymbol{\theta}) - y_i \leq T_{high,i} \quad (2)$$

The combined uncertainty probability distribution function $f_{U_{C,i}}(\epsilon_{c,i})$ is used to determine threshold bounds for every location i. They delimit the shortest intervals that contain simultaneously a target probability φ and satisfying Eq. 3. The value φ is the target reliability of the data interpretation. This is the probability that the correct model remains in the candidate model set after falsification. The definition of threshold bounds also uses the Sidak correction, which takes into account the effects of multiple measurements in the comparison of models (Sidak, 1971). This procedure has the advantage of providing conservative threshold bounds, regardless of the interdependencies between uncertainties (JCGM, 2011).

$$\forall i \in \{1, \dots, n_m\}: \varphi^{\frac{1}{n_m}} = \int_{T_{low,i}}^{T_{high,i}} f_{U_{C,i}}(\epsilon_{c,i}) d\epsilon_{c,i} \quad (3)$$

After falsification, the remaining models compose the candidate model set that instantiation of the identified parameters $\boldsymbol{\theta}^*$. This models are compatible with all measurements while accounting for modelling and measurement uncertainties. Remaining-fatigue-life provisions are then based on the predictions of the candidate model set.

Prognosis Methodology

Instead of basing remaining-fatigue-life predictions on a single model class and on a single set of parameter values, all candidate models identified are employed to calculate lower and upper bounds for predicted values.

For fatigue prognosis, the number of cycles to failure are evaluated based on the number of cycles under constant stress-range level. The stress-range predictions of each candidate models are combined with the

modelling uncertainties. The number of cycles to failure for the n_{cc} critical connections is determined using the S-N curve of the appropriate detail category given in the codes (SIA 263, 2003). This process is achieved by a Monte-Carlo analysis using one million samples. Eq. 4 presents the calculation of a sample of the number of cycles of the critical connection j.

$$\forall j \in \{1, \dots, n_{cc}\}: N_{f,j} = C \cdot \left(\Delta g_j(\boldsymbol{\theta}^*) - \Delta\epsilon_{model,j}\right)^{-m} \quad (4)$$

$\Delta g_j(\boldsymbol{\theta}^*)$ is the stress-range prediction obtained using a candidate model. $\Delta\epsilon_{model,j}$ is a sample of the stress-range modelling uncertainty. C and m are constant values that are related to the S-N curve and the detail category. For the probability distribution of the number of cycles, a prediction interval is determined for a prediction reliability of φ_{pred}, representing the shortest interval for which the probability content reaches the reliability value.

By reducing uncertainties related to the prediction of the number of cycles, the reserve capacity of the structure is quantified more accurately. In the following section, an application of this methodology is presented.

TRUSS-BEAM EXAMPLE

In this section, the prognosis methodology is applied to a steel beam composed of a circular hollow-section truss. This beam is subjected to a fatigue-load test in laboratory conditions. Figure 1 shows the geometry of the simply-supported beam with the position of the displacement gauge D1 and 36 strain gauges that are numbered between 1 and 45. Truss beam is made of standardized laminated ROR profiles. The diagonals are welded to the upper and lower chord edge surface. The beam span is 8621 mm long between the support-plate edges and its height is 1800 mm. The upper chord is simply supported on the plate and is also tied up using straps to prevent an uplift during the cyclic load test. The support plates are 150 mm large and their edges are 40 mm distant from the end-diagonal weld toe. Although there is no clear information about the strap positions, they are assumed to lie on the support plates. A cyclic load of amplitude 550 kN is applied on the top-middle of the beam.

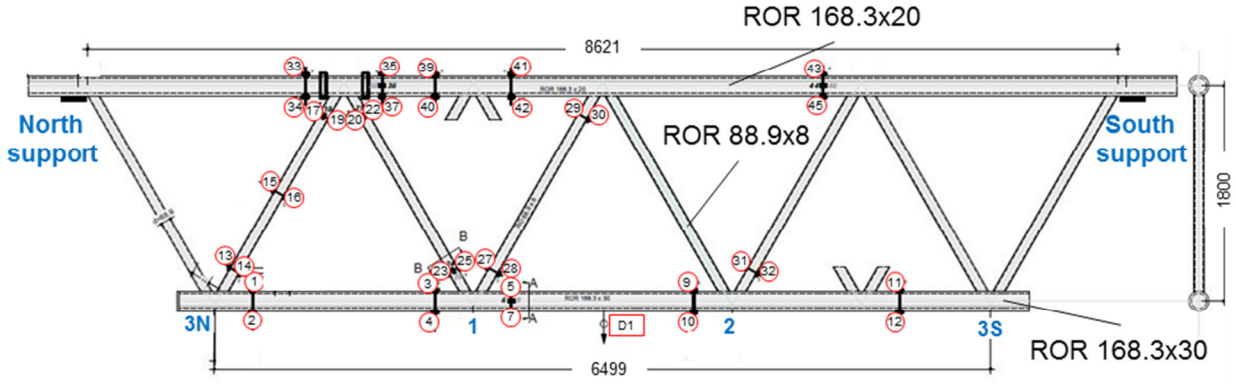

Figure 1. Truss-beam description (dimensions in *mm*)

In this example, the measurements of an initial load test are used to identify the true structural behaviour of the beam. Several unknown characteristics of the structure, such as the Young's modulus of steel and the rotational stiffness of the welded connections, are parameterised. The analysis of measurement data, which are provided by Acevedo (2011), shows differences between the values of symmetrically positioned strain gauges, as shown in Table 1. The highest relative difference is observed on the gauges located on the upper chord (#35 and #43, #37 and #45, see Figure 1). This means that asymmetrical boundary conditions have to be considered in order to find compatibility between model predictions and measurements. This is achieved by modelling rotational springs at the supports in order to consider the rotational constraint created by the lever arm between the strap and the actual contact region of the chord with the support plate. In addition, the uncertain position of the strap and the contact region of chord is modelled by two supplementary parameters. These parameters and their possible range values are given in
Table 2. Each combination of parameter values is an instantiation of the initial model set, which is composed of 24'500 model instances. Figure 2 describes the finite-element model and the parameters that are used for data interpretation.

Table 1. Measured strain during initial load test (Acevedo 2010)

Symmetric strain-gauge pairs	Measured strain pairs [$\mu\varepsilon$]	Differences relative to second strain value
5, 9	114, 110	4%
7, 10	373, 375	-1%
23, 32	620, 602	3%
25, 31	847, 840	1%
35, 43	-326, -284	13%
37, 45	-231, -262	-13%

Table 2. Initial-model-set parameter ranges and their discretization intervals

Parameter θ	Units	Range	Number of discretization intervals
Young's modulus of steel	GPa	207-210	4
Rotational stiffness of truss connections	MNm/rad	0.1-1000	5
Rotational stiffness of the south support	MNm/rad	0.1-1000	5
Rotational stiffness of the north support	MNm/rad	0.1-1000	5
South support drift	mm	0-150	7
North support drift	mm	0-150	7

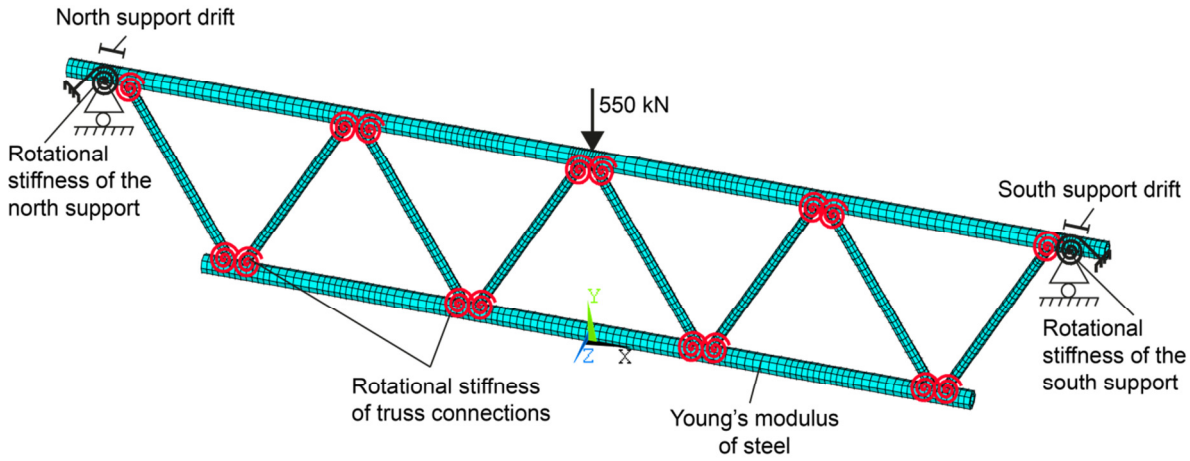

Figure 2. Finite-element model of the truss beam and parameter description

Values for $U_{model,i}$ and $U_{measure,i}$ are estimated based on uncertainty sources and their probability density function (PDF) shown in Table 3. These values are determined using field data and by engineering experience. The values for the variability of the profile dimensions are given by steel code specifications (SZS, 2005) and the uncertainty is evaluated through model-prediction variance using Monte-Carlo simulations.

Table 3. Uncertainty sources and their estimated probability density function

Uncertainty source	Units	PDF	Min	Max
Profile thickness variability	%	Uniform	-12.5	12.5
Profile diameter variability	%	Uniform	-1	1
Sensor resolution (displacement gauge)	mm	Uniform	-0.2	0.2
Sensor resolution (strain gauge)	μmm/mm	Uniform	-2	2
Cable losses	%	Uniform	-0.25	0.25
Model simplifications	%	Uniform	0	5

These uncertainties are combined and the threshold bounds are calculated for a target reliability $\varphi = 95\%$. Based on the comparison of 34 measurements, error-domain model falsification reveals a set of 107 candidate models.

These candidate models are used to calculate stress-range predictions for each critical connection on the beam lower chord that is acting in tension. Using a Monte-Carlo analysis, these predictions are combined with the stress-range modelling uncertainty $\Delta\epsilon_{model,j}$ as described in Eq. 4. This uncertainty does not account for the profile-dimension variability that are already included explicitly by S-N design curves. Thus, this uncertainty is composed of the model simplifications exclusively. Prediction intervals are derived from the probability distribution of the number of cycles to failure for a prediction reliability $\varphi_{pred} = 95\%$. Figure 3 presents the comparison of the prediction intervals for the initial model set and the candidate model set as well as the predictions for positions #3N, #1, #2 and #3S determined using a design model that is used in Acevedo (2011). This model is based on conservative assumptions such as pinned connections and the a-priori symmetrical behaviour of the beam with 0-values for drifts and support-spring stiffnesses, as well as 210 GPa for the Young's modulus of steel.

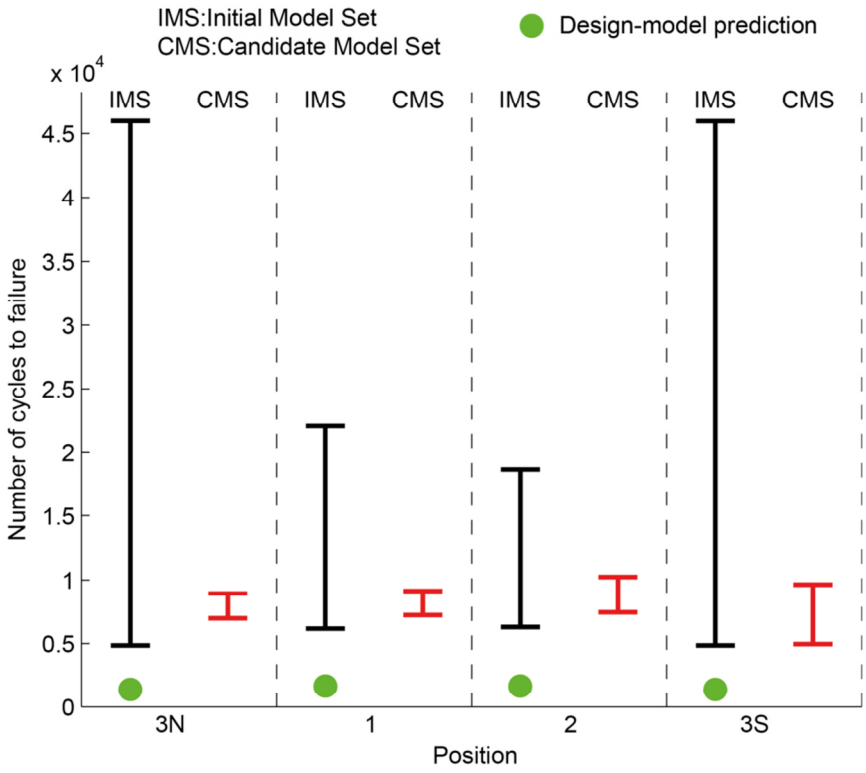

Figure 3. Comparison of the number-of-cycles-to failure predictions between the initial model set (IMS) and the candidate model set (CMS), as well as predictions made using a design model for positions #3N, #1, #2 and #3S, see Figure 1 (Acevedo, 2011)

The results show a lower number of cycles for connections #3N and #3S than for connections #1 and #2 in agreement with the observations made during the fatigue-load test. The prediction intervals for connections #3N and #3S calculated using the initial model set is larger than the intervals for connections #1 and #2. This reveals a high variability of the predictions of those connections that are located at each end of the beam. This is due to the uncertainty that is mainly located at the boundary conditions that are next to connections #3N and #3S.
By comparing the IMS-prediction interval and the CMS-prediction interval, a relative uncertainty reduction up to 95% for connection #3N (see Table 4) is observed. The relative reduction is determined based on the relative difference between the interval lengths. Because of the higher uncertainty of the end connections than of the centred connections, the relative reduction of uncertainty is higher for those connections.

In addition, the comparison of the lower bound of CMS-predictions with the design-model predictions reveals an improvement of the remaining fatigue life up to 402% (see Table 4). This percentage is based on the relative difference between the CMS-lower prediction and the design-model prediction. Figure 3 presents a greater improvement for connections #3N than for the other connections. However, this does not mean that connections, for which the predictions are the most uncertain, are connections, for which the predictions are improved the most. Indeed, predictions of connection #3S is the second most uncertain and shows the least remaining-fatigue-life improvement.

Table 4. Relative reduction and remaining-fatigue-life prediction improvement for each critical connection

	3N	**1**	**2**	**3S**
Relative reduction [%]	**95**	**88**	**77**	**89**
CMS-predictions lower bound	6979	7238	7454	4958
Design-model predictions	1390	1671	1671	1390
Prediction improvement [%]	**402**	**333**	**346**	**257**

Thus, the gain of information provided by measurement data contributes to enhance the accuracy of the remaining-fatigue-life prediction. Model-based data-interpretation techniques are also able to improve remaining-fatigue-life prognoses from those that are based on conservative models. Moreover, the initial-model-set prediction intervals reveal a great sensitivity of the remaining-fatigue-life provisions to modelling uncertainties.

CONCLUSIONS

This paper presents a methodology that improves the remaining-fatigue-life evaluation of structures. This methodology is applied to a steel beam composed of a circular-hollow-section truss. Using measurement data originating from a fatigue-load test, this application leads to the following conclusions:

- The remaining-fatigue-life accuracy is improved up to 95% in comparison with the initial-model-set predictions.
- The remaining-fatigue-life predictions are enhanced up to 402% in comparison with design-model predictions.
- As expected, the prediction accuracy is very sensitive to modelling uncertainties.

ACKNOWLEDGMENTS

The authors acknowledge J.-A. Goulet for discussions and ICOM (Steel Structures Laboratory), EPFL (A. Nussbaumer and C. Acevedo) for providing test results.

REFERENCES

Acevedo, C. (2011). *Influence of Residual Stresses on Fatigue Response of Welded Tubular K-joints*, PhD thesis 5056, EPFL, Lausanne.

ASME (2006). "Guide for verification and validation in computational solid mechanics", *ASME.*

Cheung, S.H & Beck, J.L. (2009). "Bayesian model updating using hybrid Monte Carlo simulation with application to structural dynamic models with many uncertain parameters", *Journal of Engineering Mechanics,*135(4), 243-255.

Goulet, J.-A. and Smith, I.F.C. (2011). "Prevention of over-instrumentation during the design of a monitoring system for static load tests", *In 5th International Conference on Structural Health Monitoring on Intelligent Infrastructure (SHMII-5).* Cancun, Mexico.

Goulet, J.-A. and Smith, I.F.C. (2013). "Predicting the usefulness of monitoring for identifying the behavior of structures", *Journal of Structural Engineering***,** in press.

Guo, T, Frangopol, D.M, Chen, Y. (2012). "Fatigue reliability assessment of steel bridge details integrating weigh-in-motion and probabilistic finite element analysis", *Computers & Structures,* 112:245-257.

JCGM (2011). "Evaluation of measurement data - Supplement 2 to the *"Guide to the expression of uncertainty in measurement"* - Extension to any number of output quantities", *JCGM Working Group of the Expression of Uncertainty in Measurement,* JCGM 102**,** 72p.

Liu, M., Frangopol, D.M., Kwon, K. (2010). "Fatigue reliability assessment of retrofitted steel bridges integrating monitored data, *Structural Safety,* 32(1):77-89.

Papadimitriou, C., Fritzen, C.-P., Kraemer, P., Ntotsios, E. (2011). "Fatigue predictions in entire body of metallic structures from a limited number of vibration measurements using Kalman filtering", *Structural Control and Health Monitoring*, 18, 554-573.

SIA 263 (2003). "Norme SIA 263: Steel structures", *Société suisse des ingénieurs et des architectes (SIA),* Zurich.

Sidak, Z. (1971). "On probabilities of rectangles in multivariate Student distributions: their dependence on correlations", *The Annals of Mathematical Statistics***,** 169-175.

Siriwardane, S., Ohga, M., Dissanayake, R., Taniwaki, K. (2008). "Application of new damage indicator-based sequentual law for remaining fatigue life estmation of railway bridges", *Journal of Constructional Steel Research,* 64(2):228-237.

Strauss, A., Frangopol, D.M., Kim, S. (2008). "Use of monitoring extreme data for the performance prediction of structures: Bayesian updating", *Engineering Structures,* 30(12), 3654-3666.
SZS (2005). "Konstruktionstabellen. C5/05 steel work", *Stahlbau Zentrum Schweiz.* 130p.
Zhang, E.L., Feissel, P., Antoni, J. (2011). "A comprehensive Bayesian approach for model updating and quantification of modelling errors", *Probabilistic Engineering Mechanics,* 26(4), 550-560.